



Systemic *Candida albicans* Infection in Mice Causes Endogenous Endophthalmitis via Breaching the Outer Blood-Retinal Barrier

Sneha Singh,^a Sukhvinder Singh,^a  Ashok Kumar^{a,b}

^aDepartment of Ophthalmology, Visual and Anatomical Sciences/Kresge Eye Institute, Wayne State University School of Medicine, Detroit, Michigan, USA

^bDepartment of Biochemistry, Microbiology, and Immunology, Wayne State University School of Medicine, Detroit, Michigan, USA

ABSTRACT *Candida albicans* is the leading cause of endogenous fungal endophthalmitis; however, its pathobiology studies are limited. Moreover, the contribution of host factors in the pathogenesis of *Candida* endophthalmitis remains unclear. In the present study, we developed a murine model of *C. albicans* endogenous endophthalmitis and investigated the molecular pathobiology of ocular candidiasis and blood-retinal barrier permeability. Our data show that intravenous injection of *C. albicans* in immunocompetent C57BL/6 mice led to endogenous endophthalmitis without causing mortality, and *C. albicans* was detected in the eyes at 3 days postinfection and persisted for up to 10 days. The intraocular presence of *C. albicans* coincided with a decrease in retinal function and increased expression of inflammatory mediators (tumor necrosis factor alpha [TNF- α], interleukin 1 β [IL-1 β], MIP2, and KC) and antimicrobial peptides (human β -defensins [hBDs] and LL37) in mouse retinal tissue. *C. albicans* infection disrupted the blood-retinal barrier (BRB) by decreasing the expression of tight junction (ZO-1) and adherens junction (E-cadherin, N/R-cadherin) proteins. *In vitro* studies using human retinal pigment epithelial (ARPE-19) cells showed time-dependent activation of eIF2 α , extracellular signal-related kinase (ERK), and NF- κ B signaling and decreased activity of AMP-activated protein kinase (AMPK) leading to the induction of an inflammatory response upon *C. albicans* infection. Moreover, *C. albicans*-infected cells exhibited increased cellular permeability coinciding with a reduction in cellular junction proteins. Overall, our study provides new insight into the molecular pathogenesis of *C. albicans* endogenous endophthalmitis. Furthermore, the experimental models developed in the study can be used to identify newer therapeutic targets or test the efficacy of drugs to treat and prevent fungal endophthalmitis.

IMPORTANCE Patients with candidemia often experience endophthalmitis, a blinding infectious eye disease. However, the pathogenesis of *Candida* endophthalmitis is not well understood. Here, using *in vivo* and *in vitro* experimental models, we describe events leading to the invasion of *Candida* into the eye. We show that *Candida* from the systemic circulation disrupts the protective blood-retinal barrier and causes endogenous endophthalmitis. Our study highlights an important role of retinal pigment epithelial cells in evoking innate inflammatory and antimicrobial responses toward *C. albicans* infection. This study allows a better understanding of the pathobiology of fungal endophthalmitis, which can lead to the discovery of novel therapeutic targets to treat ocular fungal infections.

KEYWORDS *Candida albicans*, endogenous endophthalmitis, fungal endophthalmitis, inflammation, retina, eye, blood-retinal barrier, endophthalmitis, innate immunity

Infectious endophthalmitis is a vision-threatening eye infection (1–3). Among various pathogens, fungi are the second leading cause of exogenous and endogenous endophthalmitis after bacteria, wherein the microbe gains access to the ocular tissue

Editor Damian J. Krysan, University of Iowa Hospitals and Clinics

Copyright © 2022 Singh et al. This is an open-access article distributed under the terms of the [Creative Commons Attribution 4.0 International license](https://creativecommons.org/licenses/by/4.0/).

Address correspondence to Ashok Kumar, akuma@med.wayne.edu.

The authors declare no conflict of interest.

Received 8 May 2022

Accepted 15 July 2022

Published 1 August 2022

via an external source of contamination or the hematogenous route, respectively (4, 5). *Candida* is the most common causative agent of endogenous fungal endophthalmitis in hospitals, with *C. albicans* being the most prevalent species (6–10). *C. albicans* is a commensal pathogen inhabiting the oral, gastrointestinal, and genital tracts, which, upon disruption of the protective barrier or alteration of the host immune response, can enter the bloodstream and cause infection (11). In addition to systemic infections, *C. albicans* can cause ocular candidiasis in approximately 10% to 25% of candidemia patients (1, 7, 12, 13). The *Candida* endogenous endophthalmitis is mainly associated with immunocompromised or immunosuppression conditions; however, *C. albicans* can also cause endophthalmitis in immunocompetent individuals (14–16).

Most studies related to *Candida* endophthalmitis are classified as clinical and epidemiological, where the focus of the study is to describe the risk factors (parenteral nutrition; immunosuppression; intravenous drug use; recent central venous catheters, including peripherally inserted central catheters; race; and age) involved in the pathogenesis (1, 7, 12, 13, 17). Surprisingly, the few experimental studies available (13, 18–21) have an emphasis on evaluating the efficacy of antifungal drugs and comparing the infectivity of different *Candida* species. Previously, we have established a murine model of *Aspergillus* and *Candida* endophthalmitis to characterize the retinal innate immune response and its pathogenesis (4, 22). However, in these studies, fungi were administered via intravitreal injections, representing the exogenous endophthalmitis models.

C. albicans infection was significantly associated with ocular candidiasis due to its enhanced capacity for tissue invasion, inflammation, and recruitment of neutrophils (4, 13). However, it is important to note that not every candidemia patient develops endophthalmitis. This is because the eye is protected from inflammatory cells and pathogen invasion by the blood-retinal barrier (BRB), composed of retinal pigment epithelium (outer BRB) and retinal endothelium (inner BRB) (23). The tight and adherens junction protein binds the BRB intracellular junctions to maintain the barrier integrity (24). Dysfunction or degradation of these junction proteins can lead to a breach of the BRB and contribute to endogenous endophthalmitis and loss of retinal function. Currently, the interactions of *Candida* with BRB cells remain elusive, as suitable experimental models are needed to study the pathogenesis of endogenous *Candida* endophthalmitis. We postulate that intracellular junction disruption and BRB permeability precedes *C. albicans* endogenous endophthalmitis.

Here, we sought to develop a murine model of endogenous *C. albicans* endophthalmitis using systemic routes of infection along with the characterization of its pathogenesis. The *in vivo* study was complemented with an *in vitro* model of *C. albicans* infection of human retinal pigment epithelial cells, constituting the outer BRB. Hence, the development of appropriate experimental models and an in-depth understanding of pathological changes during *C. albicans* endophthalmitis can lead to the identification of novel therapeutics to prevent fungal endophthalmitis.

RESULTS

Systemic *Candida* infection results in endogenous endophthalmitis in mice.

Endogenous endophthalmitis is caused by the hematogenous spread of *C. albicans* in candidemia patients (14–16). To mimic the clinical scenario of systemic infection, we injected *C. albicans* into immunocompetent C57BL/6 (B6) mice via intravenous (i.v.) and intraperitoneal (i.p.) routes and assessed intraocular fungal burden, electroretinography (ERG) response, and inflammatory mediators (Fig. 1A). We observed that i.v. and i.p. injections of $\sim 5 \times 10^5$ CFU of *C. albicans* led to its dissemination in multiple mouse organs (liver, spleen, and kidney), including the eye assessed at day 3 (D3) postinjection. However, the fungal burden was lower in the eyes than in other organs (Fig. 1B). Moreover, the i.v. route of inoculation resulted in a relatively higher *C. albicans* burden than the i.p. route. The presence of *C. albicans* in the eye coincided with a 20% to 30% reduction in ERG response as measured in terms of a-wave and b-wave amplitudes (Fig. 1C).

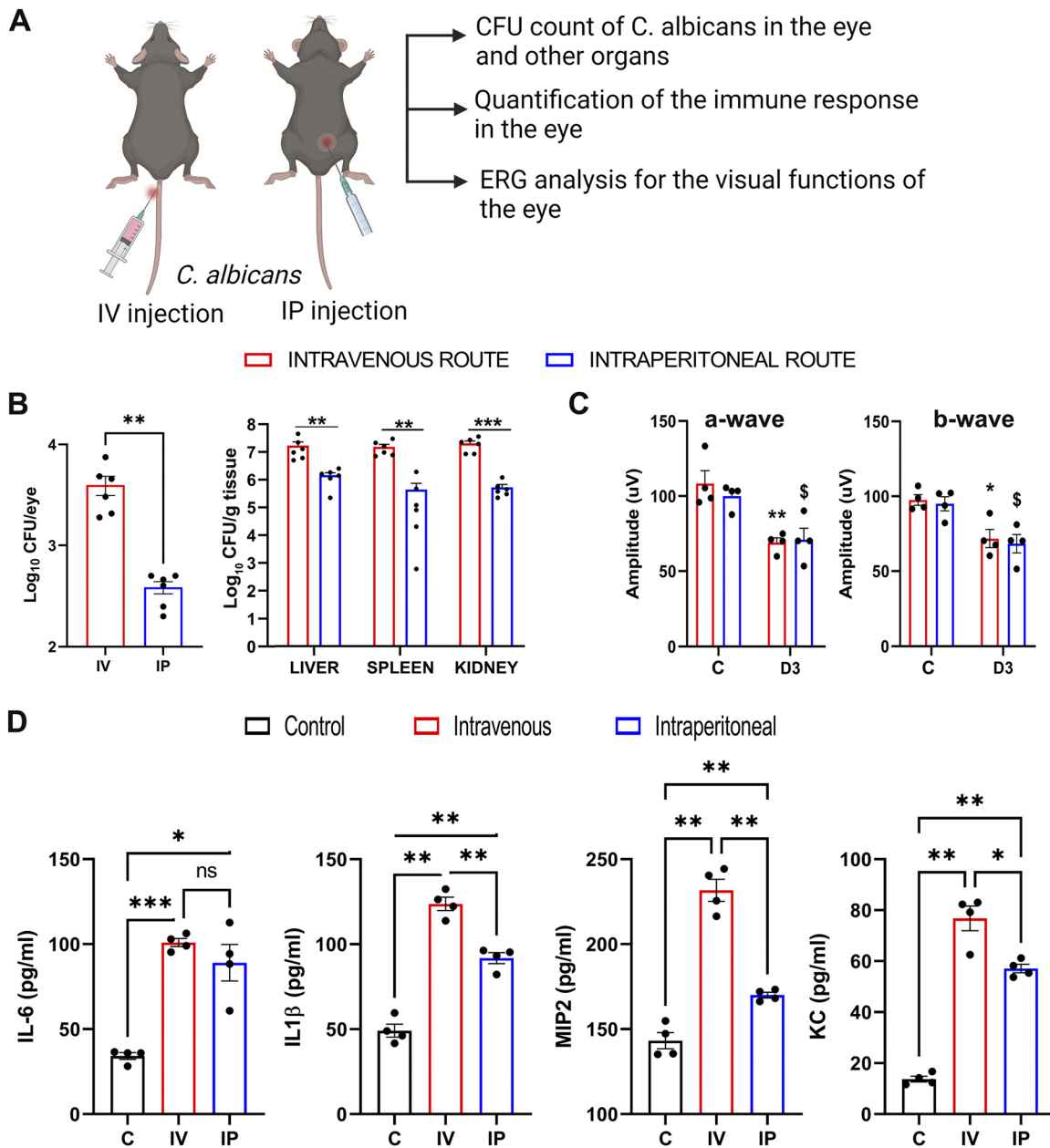


FIG 1 Systemic *C. albicans* infection causes endophthalmitis in C57BL/6 mice. (A) Schematic representation of the experimental setup showing intravenous or intraperitoneal injection of $\sim 5 \times 10^5$ CFU of *Candida albicans* in C57BL/6 mice ($n = 4$ to 6). (B) The eyes and indicated organs were harvested at 3 days (D3) postinfection, and fungal burden was estimated by the standard plate count method. (C and D) In another experiment, at D3, ERG response was measured in anesthetized mice ($n = 4$) (C), and enucleated whole-eye lysates were used to assess indicated inflammatory mediators by ELISA (D) and expressed as picogram per milliliter. ns, nonsignificant; *, $P < 0.05$; **, $P < 0.01$; ***, $P < 0.001$. Unpaired *t* test was used in panel B, one-way analysis of variance (ANOVA) and Šidák's multiple-comparison test in panel C, and Dunnett's multiple-comparison test in panel D. *, control versus i.v.; \$, control versus i.p. (C).

One of the hallmarks of endophthalmitis is the induction of intraocular inflammation. To this end, our data showed that *C. albicans*-infected eyes had increased levels of the inflammatory mediators interleukin 6 (IL-6), IL-1β, MIP2, and KC (Fig. 1D). Interestingly, the i.v. route of *C. albicans* administration induced a higher inflammatory response in the eye than that injected via i.p.

Since fungal infections are more prevalent in immunocompromised individuals, most experimental models have utilized immunosuppressive approaches to study the pathogenesis of fungal infections (25). However, the immunocompromised status tends to

have increased mortality in animal models. In contrast, our data showed that intravenous injection of *C. albicans*, ranging from 10^4 to 10^7 CFU, did not cause mortality in immunocompetent mice observed for up to 10 days (see Fig. S1A in the supplemental material). The gross examination of kidneys showed abscess formation, but *C. albicans* burden was drastically reduced in all groups, with significant numbers of kidneys showing no viable *C. albicans* growth at 10 days postinfection (dpi) (Fig. S1B). In contrast, *C. albicans* was present in eyes of all experimental groups, even at 10 dpi (Fig. S1C).

Collectively, these results show that *C. albicans* can invade immunocompetent mice eyes during systemic infection and cause endophthalmitis. Moreover, the i.v. route of *C. albicans* administration results in a higher fungal burden and ocular pathology. Thus, we decided to choose the i.v. route of *C. albicans* injection for the rest of the study.

***C. albicans* induces activation of inflammatory signaling in the mouse retina.**

Foregoing results show the invasion of *C. albicans* in mouse eyes on day 3. Next, we performed a time course study and observed that *C. albicans*-infected eyes had increased levels of inflammatory cytokines (MIP2, IL-6, tumor necrosis factor alpha [TNF- α], and IL-1 β) on both day 3 and day 6 postinjection, with relatively higher levels at day 6 (Fig. 2A). As the enzyme-linked immunosorbent assay (ELISA) was performed on the whole-eye lysates, various ocular tissues may be contributing to the overall inflammatory response. However, during endogenous endophthalmitis, the main tissue affected is the retina and vitreous chamber. Thus, we assessed the effect of systemic *C. albicans* infection on mouse retinal tissue. We found that in comparison to uninfected control (C) eyes, the retinal tissue of *C. albicans*-infected mice exhibited activation of inflammatory signaling molecules (Fig. 2B). Our data showed a time-dependent increase in both pro- and active IL-1 β levels. This coincided with an increase in levels of p-NF- κ B, p-ERK, and p-eIF2 α and the downregulation of p-AMPK α (Fig. 2C). Overall, significant changes were observed on day 3 and day 6 post-*C. albicans* injection. One of the outcomes of activation of NF- κ B and mitogen-activated protein kinase (MAPK) signaling is the transcription and production of inflammatory mediators. Our quantitative PCR (qPCR) analysis revealed a time-dependent increase in the expression of inflammatory cytokines (e.g., IL-6, IL-1 β , TNF- α , and CXCL2), cell activation markers (e.g., *Icam1*), and proangiogenesis growth factors (e.g., *Fgf-2*) transcripts in *C. albicans*-infected mouse retinal tissue (Fig. 2D). Together, these results indicate that systemic *C. albicans* infection evokes an inflammatory response in the retina.

Systemic *C. albicans* infection impairs the outer blood-retinal barrier. Being an immune-privileged organ, the eye is protected from systemic pathogen circulation by the presence of the blood-retinal barrier (BRB). Our data showing the presence of *C. albicans* in the eye and the induction of inflammatory response in the mouse retina indicate the possibility of the breach of BRB. To test this, mice were injected with *C. albicans* via the i.v. route and on day 3 and day 6 postinjection, Evans blue dye (0.5%) was infused, and following the perfusion, the accumulation of the dye was assessed in various organs (Fig. 3A). Our data show that *C. albicans*-infected mice eyes had increased levels of Evans blue dye both on day 3 and day 6 (Fig. 3B). A similar accumulation of the dye was observed in other organs (e.g., spleen, liver, and kidney), but at relatively higher concentrations than in the eye.

Because several intracellular junction proteins maintain the BRB, we assessed the effect of *C. albicans* infection on these junction proteins by analyzing retinal tissue on day 3 and day 6 post-*C. albicans* injection. Our data showed a reduction in protein levels of ZO-1, N/R-cadherin, and E-cadherin in *C. albicans*-infected mouse retinal tissue by Western blot analysis (Fig. 3C and D). Overall, these results imply that *C. albicans* can gain access to the eye by downregulating cell junction proteins of the BRB.

BRB is maintained by retinal endothelial cells and retinal pigment epithelial (RPE) cells constituting the inner and outer BRB, respectively (23). Given the downregulation of ZO-1, abundantly expressed in RPE, we postulated the potential breach of outer BRB in our model. To determine the role of RPE cells in our model, mice were injected with sodium iodate (NaIO₃) 24 h prior to systemic *C. albicans* infection. NaIO₃ treatment compromises the outer BRB by inducing necroptosis in RPE cells (24, 26–28), resulting

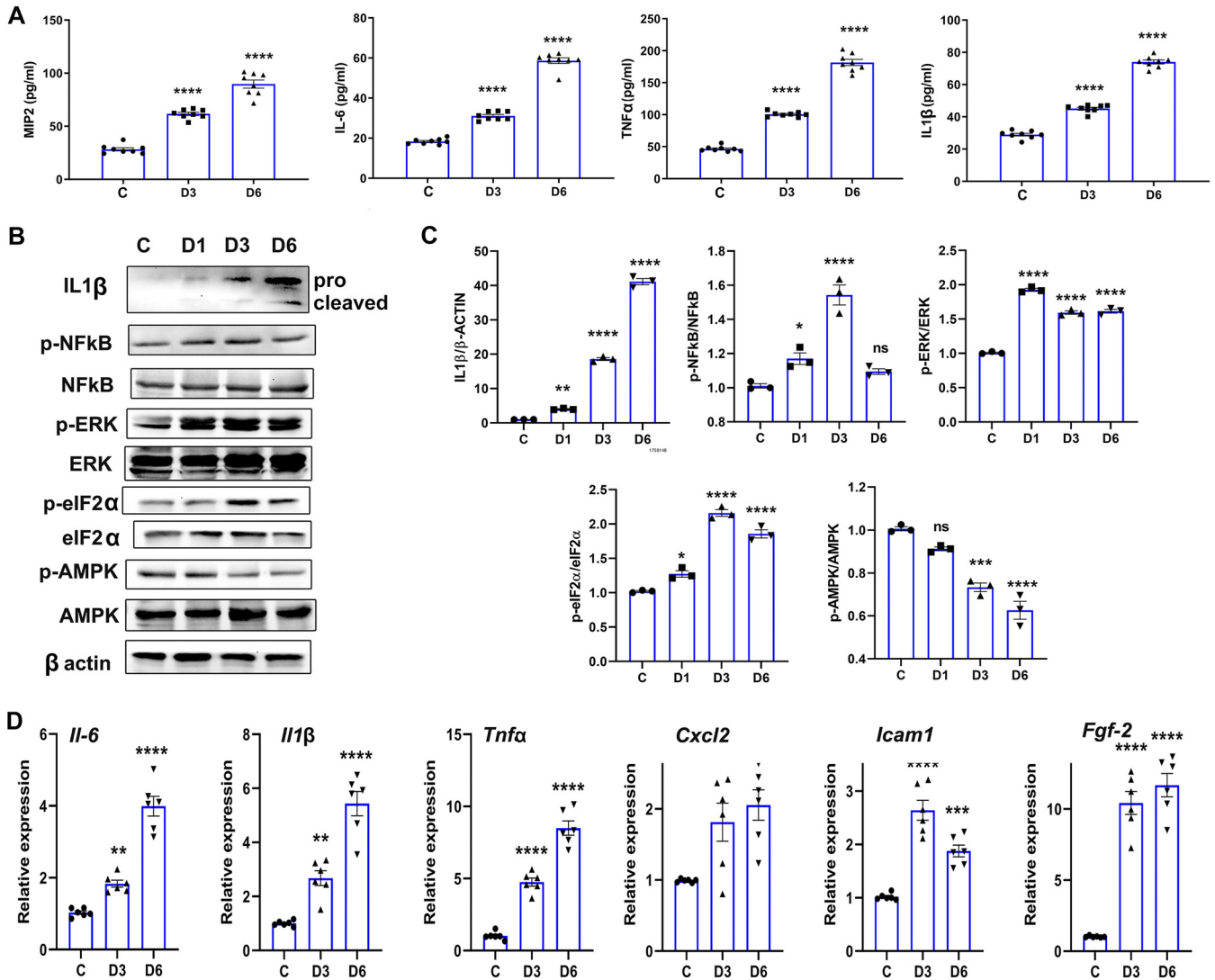


FIG 2 *C. albicans*-infected eyes exhibit an inflammatory response in the retina. (A) C57BL/6 mice ($n = 8$) were infected with *C. albicans* ($\sim 5 \times 10^5$ CFU/mice) by the intravenous route, and eyes were enucleated on day 3 (D3) and day 6 (D6) postinfection for ELISA measurement of indicated inflammatory cytokines. In another experiment, retinal tissue was harvested from *C. albicans*-infected eyes at indicated days postinfection. (B to D) Western blotting (B) with densitometry ($n = 3$) (C) and qPCR analyses ($n = 6$) (D) were performed to assess the activation of inflammatory signaling and the expression of inflammatory response genes, respectively. Statistical analysis was performed using one-way ANOVA with Dunnett's multiple-comparison test. *, $P < 0.05$; **, $P < 0.01$; ***, $P < 0.001$; ****, $P < 0.0001$; ns, nonsignificant.

in decreased ERG response and enhanced inflammatory response (29, 30). Our data showed that intraocular fungal burden almost doubled in NaIO₃-treated, *C. albicans*-injected mice (Fig. 4A). Moreover, NaIO₃ treatment alone decreased levels of junction proteins, ZO-1, and E-cadherin in retinal tissue (Fig. 4B). The assessment of retina by ERG showed a significant decline in both a- and b-wave amplitudes in *C. albicans*-infected eyes, and reduction was higher in mice pretreated with NaIO₃ (Fig. 4C). It should be noted that NaIO₃ alone also reduced ERG response. Consistent with increased fungal burden, NaIO₃-treated, *C. albicans*-injected mice exhibited higher levels of inflammatory mediators (IL-6, IL-1β, CXCL2, and TNF-α) than *C. albicans* or NaIO₃ alone (Fig. 4D). Collectively, these findings demonstrate the ability of *C. albicans* to invade the eye by disrupting the outer BRB.

C. albicans infection induces an innate immune response in cultured RPE cells.

Our *in vivo* data indicate the involvement of outer BRB in *C. albicans* endogenous endophthalmitis. To investigate the interaction of *C. albicans* with outer BRB, we adopted the *in vitro* model of cultured RPE cells. First, we performed a dose-response study by infecting

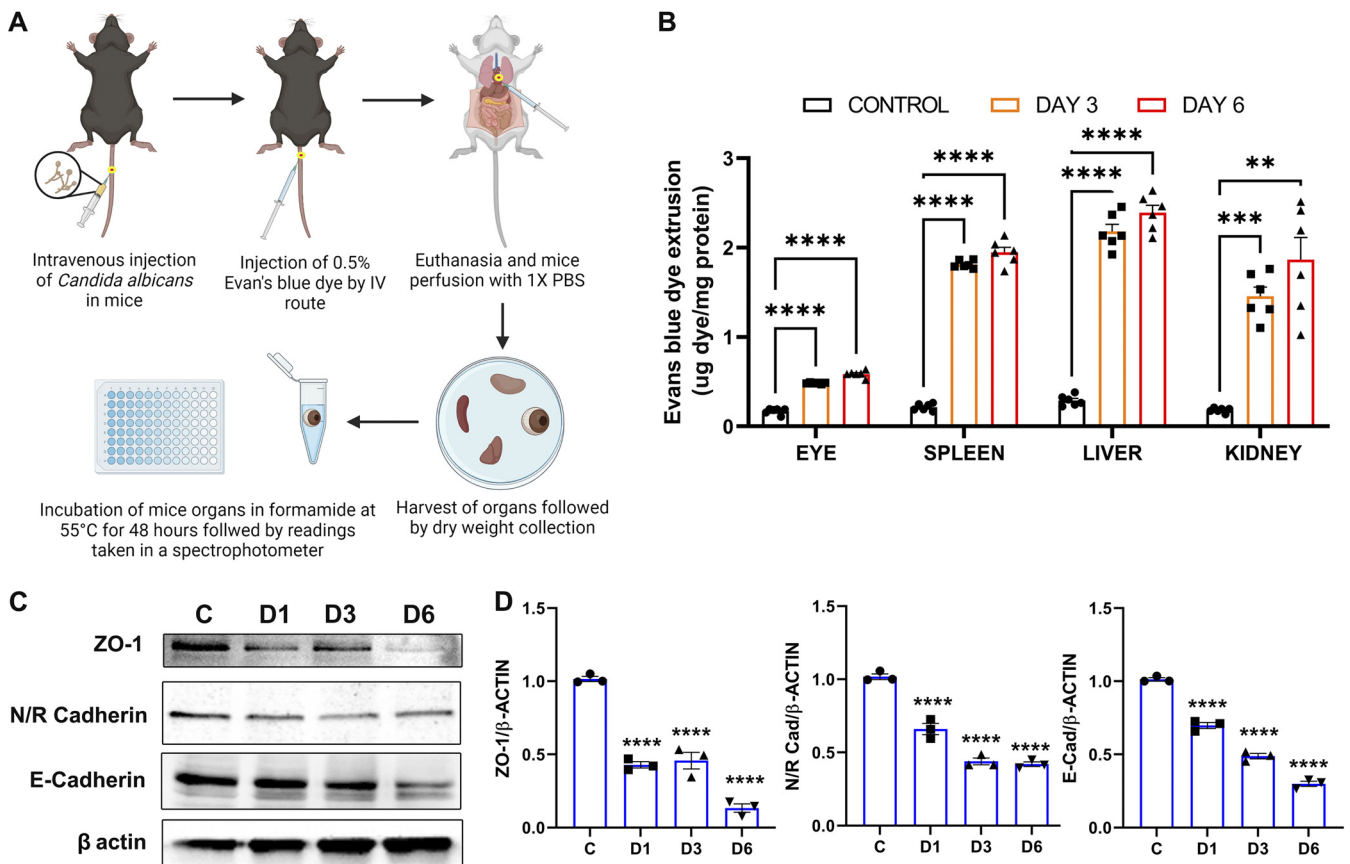


FIG 3 *C. albicans* infection breaches the blood-retinal barrier in the mouse eye. (A) C57BL/6 mice ($n = 6$) were infected with *C. albicans* ($\sim 5 \times 10^5$ CFU/mouse) by the i.v. route. On day 3 (D3) or day 6 (D6), Evans blue dye was injected via the tail vein followed by euthanasia and cardiac perfusion. (B) The eyes and indicated organs were harvested for the estimation of the quantity of dye in the tissues and expressed as μg dye/mg protein of the tissue. (C) In another experiment, *C. albicans*-injected and PBS-injected (control [C]) retinal tissue was isolated on D1, D3, and D6 and used for immunoblotting. (D) Densitometry quantification ($n = 3$) was performed and expressed as fold change with respect to the control tissues. *, $P < 0.05$; **, $P < 0.01$; ***, $P < 0.001$; ****, $P < 0.0001$; one-way ANOVA with Dunnett's multiple-comparison test.

ARPE-19 cells with *C. albicans* at various multiplicities of infection (MOIs) (0.1, 0.5, and 1) for 6 h. Our data showed dose-dependent expression of inflammatory mediators (TNF- α , IL-1 β , and IL-6) and antimicrobial peptides (human β -defensin 1 [hBD1] and hBD2) except LL-37 in *C. albicans*-infected cells (Fig. 5A). The increased levels of inflammatory cytokines were also confirmed by ELISA (Fig. 5B). As *C. albicans*-infected RPE cells exhibited the highest inflammatory response at an MOI of 1, we selected this dose for all *in vitro* experiments.

Next, we performed a time course study to assess the activation of inflammatory signaling in *C. albicans*-infected cells (Fig. 6A). To this end, our data showed a time-dependent increase in levels of both pro- and active IL-1 β and phosphorylation of NF- κ B, ERK, and eIF2 α . The activation of ERK and AMPK α showed biphasic response with modulation at 1 h and 12 h postinfection (Fig. 6B). Coinciding with the activation of NF- κ B signaling, *C. albicans*-infected RPE cells showed a time-dependent increase in the expression of inflammatory cytokines and antimicrobial peptides. However, the mRNA level of LL-37 increased early on but declined at later time points (Fig. 6C). The production of inflammatory cytokines (IL-6, IL-8, and IL-1 β) at the protein levels also showed a time-dependent increase in culture media of *C. albicans*-infected cells (Fig. 6D). These results indicate that *C. albicans* infection triggers inflammatory and antimicrobial response in RPE cells.

***C. albicans* infection increases transepithelial permeability in RPE cells.** Our *in vivo* data showed that systemic *C. albicans* infection resulted in endogenous endophthalmitis and *C. albicans* invasion into the mouse eye is increased by altering the RPE layer using NaIO₃. To further investigate the role of outer BRB during *C. albicans*

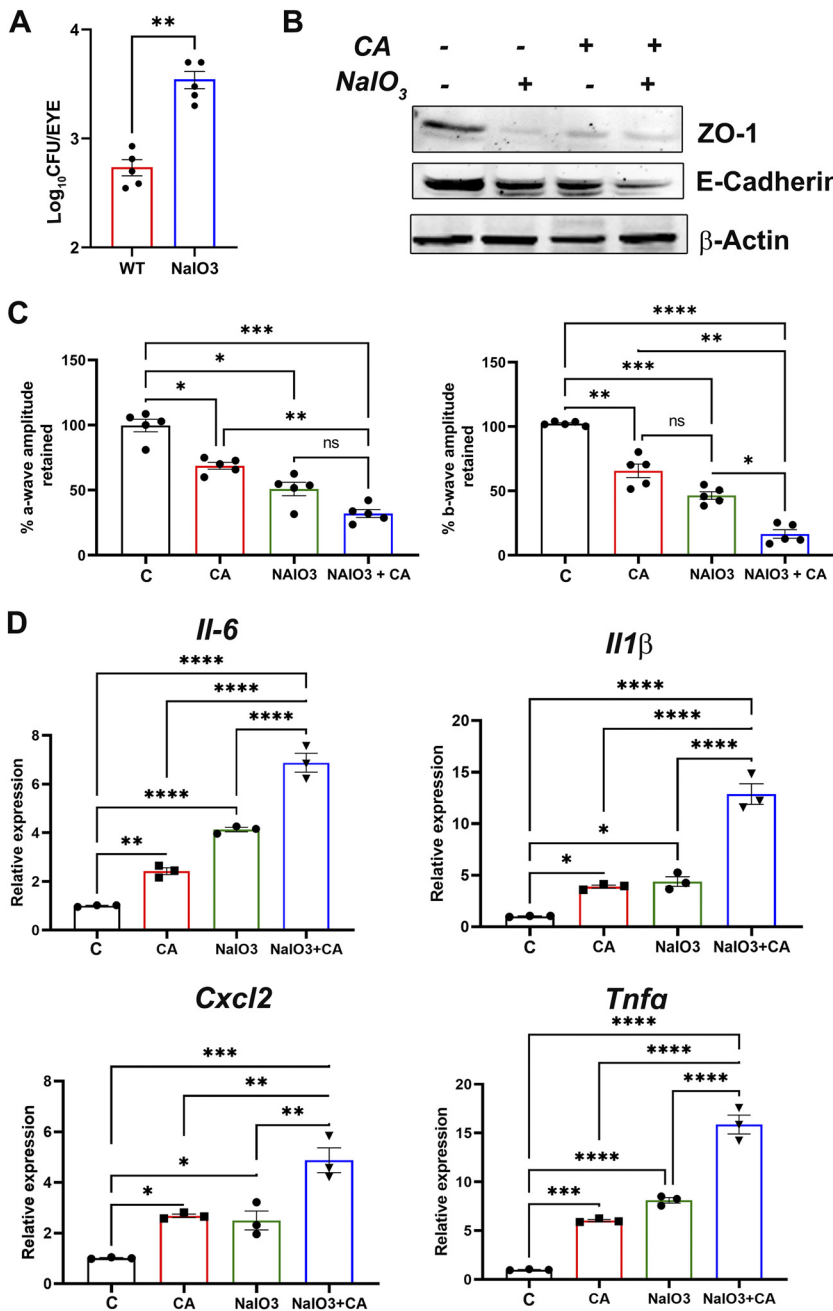


FIG 4 Disruption of outer BRB increases *C. albicans* invasion into the eye. C57/BL6 mice ($n = 4$ to 5) were pretreated with NaIO₃ (50 mg/kg) followed by i.v. injection of *C. albicans* ($\sim 5 \times 10^5$ CFU/mouse). The fungal burden in the mice eyes (A), intercellular junction protein levels (B), and the ERG response (C) were quantified on day 3 postinjection. (D) qPCR from the mice retinas ($n = 3$) was performed to assess the expression of inflammatory response genes. Statistical analysis was performed using unpaired *t* test (A) and one-way ANOVA with Tukey's multiple-comparison test (B and C). ns, nonsignificant; *, $P < 0.05$; **, $P < 0.01$; ***, $P < 0.001$; ****, $P < 0.0001$.

infection, we studied the effect of *C. albicans* infection on intracellular junction integrity using fluorescein isothiocyanate (FITC)-dextran transepithelial permeability assay. Briefly, ARPE-19 cells were seeded onto transwell culture inserts to reach confluence in 3 to 4 days and were infected with *C. albicans* at an MOI of 1. FITC-dextran was added to the upper chamber at different time points (ranging from 1 h to 24 h) post-*C. albicans* infection, and its concentrations were measured in the lower chamber (Fig. 7A). We found that *C. albicans* infection led to a significant increase in FITC-dextran

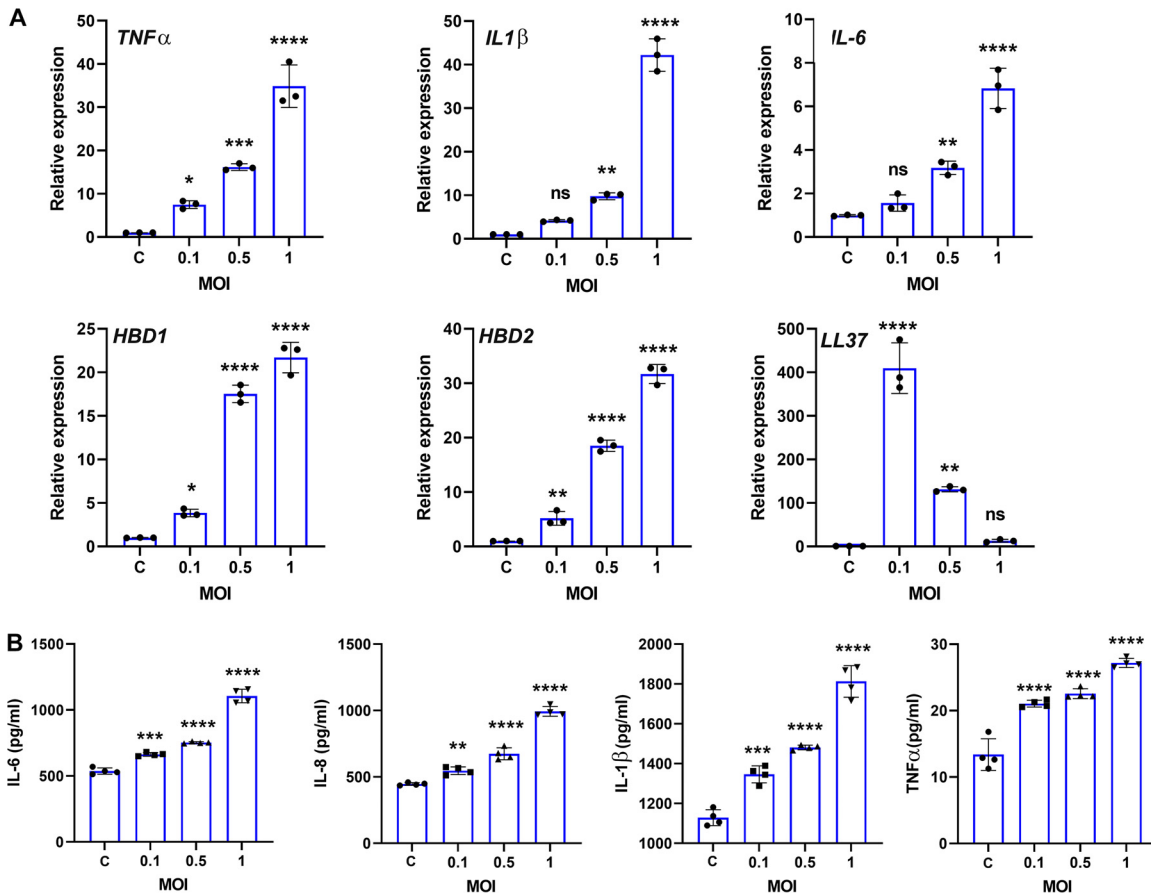


FIG 5 *C. albicans* triggers inflammatory and antimicrobial response in RPE cells. ARPE-19 cells ($n = 3$ to 4) were infected with *C. albicans* at different multiplicities of infection (MOIs) for 6 h. qPCR (A) and ELISA (B) were performed to check the expression and production of indicated inflammatory mediators. ns, nonsignificant; *, $P < 0.05$; **, $P < 0.01$; ***, $P < 0.001$; ****, $P < 0.0001$; one-way ANOVA with Dunnett’s multiple-comparison test.

permeability through the cell monolayer, and the response was time dependent, with higher levels in cells infected for 12 h (Fig. 7B). To determine whether the observed phenomenon was a result of the breakdown of intracellular junction proteins, an immunostaining assay was performed to visualize ZO-1 localization at the cellular junctions. The uninfected control ARPE-19 monolayer showed an intact cell-cell boundary stained for ZO-1, but its intensity was lost in *C. albicans*-infected cells at 3 hours postinfection (hpi) or 6 hpi (Fig. 7C) as quantified by cells with positive ZO-1 staining (Fig. 7D). The filamentous hyphae of *C. albicans* were also visible in the immunofluorescence assay (IFA) images. The decrease in the tight junction (ZO-1) and adherens junction (N/R-cadherin, and E-cadherin) proteins was confirmed by Western blot analysis (Fig. 7E). These results indicate that the increase in intracellular epithelial permeability was due to the loss of cell-cell junction proteins in the RPE cell monolayer upon *C. albicans* infection.

The foregoing results show that *C. albicans* infection impaired the outer BRB and evoked inflammatory response both *in vitro* and *in vivo*. Because both fungal cell wall (31) and secreted proteinases (32) of *C. albicans* contribute to virulence and pathogenesis, we sought to assess the effect of live and heat-killed *C. albicans* on RPE cells. First, we observed that in comparison to heat-killed *C. albicans*, live *C. albicans* infection caused significant cell death as measured by lactate dehydrogenase (LDH) release (Fig. S2A). Moreover, LDH levels increased in a time-dependent manner in live *C. albicans*-infected RPE cells (Fig. S2B). RPE cells exposed to heat-killed *C. albicans* exhibited significantly lower inflammatory and antimicrobial response than live *C. albicans* (Fig. S2C).

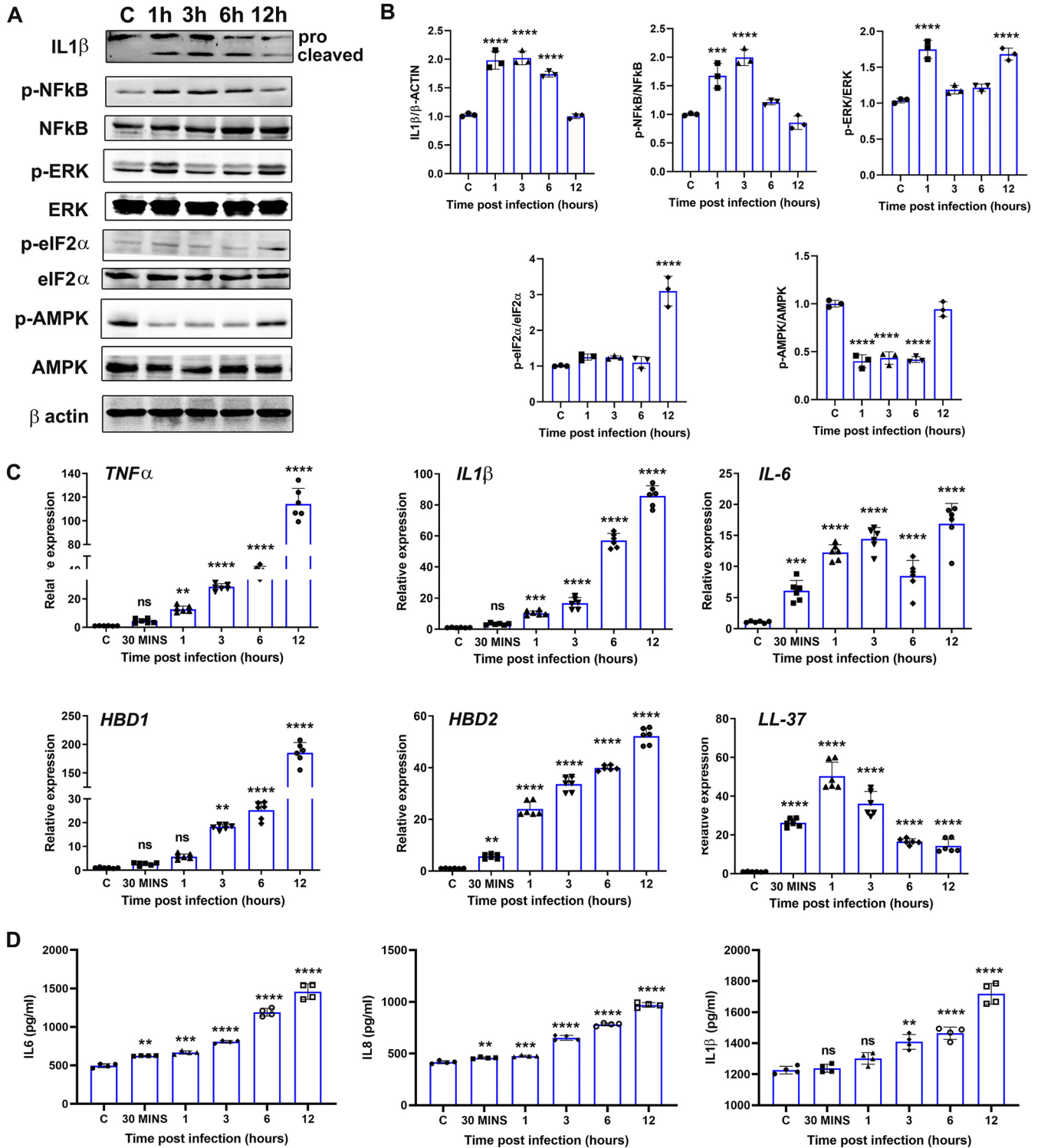


FIG 6 *C. albicans*-infected RPE cells exhibited activation of inflammatory signaling in a time-dependent manner. (A) ARPE-19 cells were infected with *C. albicans* at an MOI of 1 for different time points. Cells were used for immunoblotting (A), densitometry (B), and qPCR ($n = 6$) (C) detection of inflammatory cytokines, whereas culture supernatant ($n = 4$) was used for ELISA (D). ns, nonsignificant; *, $P < 0.05$; **, $P < 0.01$; ***, $P < 0.001$; ****, $P < 0.0001$; one-way ANOVA with Dunnett's multiple-comparison test.

The immunostaining showed disruption in membrane localization of ZO-1 in RPE cells challenged with live, but not the heat-killed, *C. albicans* (Fig. S2D). These results indicated the direct effects of *C. albicans* in inducing inflammatory response and causing loss of RPE barrier integrity.

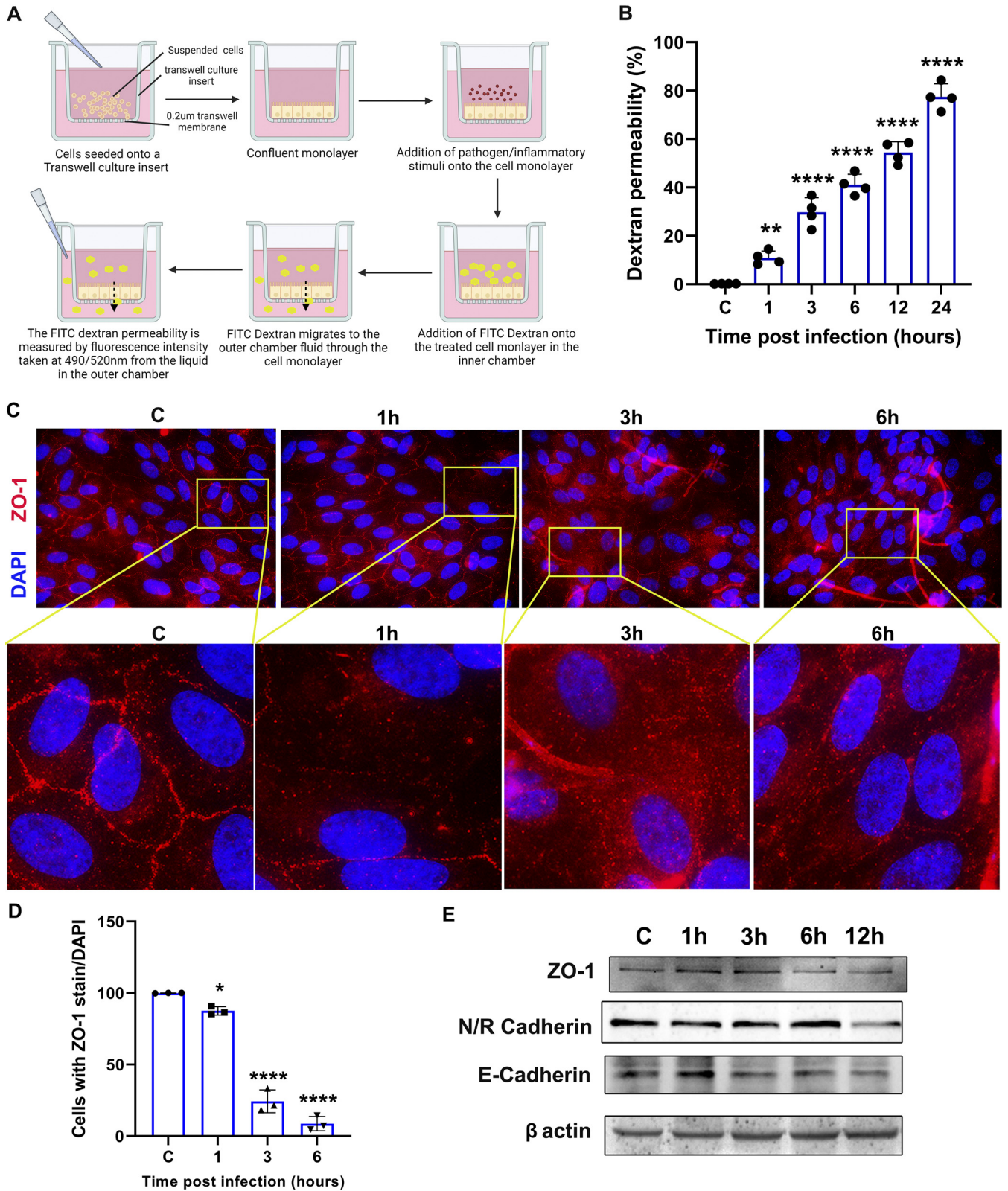


FIG 7 *C. albicans* infection decreases intracellular barrier integrity in RPE cells. (A) Schematic representation of the transwell FITC-dextran assay. (B) The dextran permeability of the *C. albicans*-infected ARPE-19 cells ($n = 4$) was expressed as percentage (%) compared to mock-infected control cells. (C) Cells infected with *C. albicans* were subjected to immunofluorescence staining to detect ZO-1 (red), and the cell nuclei were counterstained using DAPI (blue). The images were enlarged from specific regions indicated by yellow boxes. (D) The cells with complete ZO-1 staining at the cell periphery were counted with respect to the cell nuclei ($n = 3$). (E) In another experiment, *C. albicans*-infected cells were used for immunoblotting to check levels of indicated tight and adherens junction proteins. ns, nonsignificant; *, $P < 0.05$; **, $P < 0.01$; ***, $P < 0.001$; ****, $P < 0.0001$; one-way ANOVA with Dunnett's multiple-comparison test.

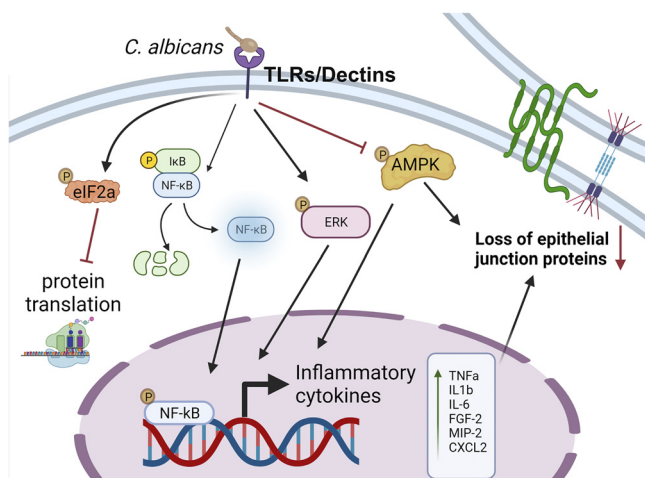


FIG 8 Schematics of *Candida* endogenous endophthalmitis pathogenesis. During systemic infection (i.e., candidemia), *C. albicans* in the choroidal blood vessels encounter RPE cells, which constitute the outer blood-retinal barrier (BRB). RPE cells recognize *C. albicans* via pathogen recognition receptors (e.g., TLRs or DECTINs) and trigger the cascade of inflammatory and stress signaling involving inflammation NF-κB, ERK, and eIF2α along with reduction in activated AMPK signaling. This results in the production of inflammatory cytokines/chemokines, which contribute toward increased cellular permeability. The figure was prepared using BioRender.

DISCUSSION

Endogenous endophthalmitis is a serious and devastating ocular infection. Due to their omnipresence, *Candida* species will continue to be the most common causative agents of endogenous fungal endophthalmitis (14–16, 33). The lack of information on host-pathogen interactions and the mechanisms of barrier property changes during ocular candidiasis have remained elusive, in part due to the lack of appropriate experimental models (4, 13, 22, 34–36). Therefore, we sought to determine the extent to which the BRB is compromised during *C. albicans* endophthalmitis by using our experimental fungal endogenous endophthalmitis murine model. Furthermore, we wanted to examine whether disruption of the cell-cell junctions comprising the ocular barrier contributed to this dysfunction. In this study, we demonstrated that systemic *C. albicans* injection in mice resulted in endogenous endophthalmitis. Our data show that *C. albicans* infection can impair the outer BRB by disrupting intracellular junction proteins in RPE cells, allowing *C. albicans* to invade the eye. Collectively, our study provides novel mechanistic insights into the pathogenesis of *C. albicans* endogenous endophthalmitis (Fig. 8).

Previous studies have used rabbit and mice models, with two routes of fungus administration, intravitreal and systemic (intravenous), to induce endophthalmitis (4, 13, 22, 34–36). Intravitreal injection directly introduces the pathogen inside the eye, causing vigorous inflammation, whereas the systemic infection in immunocompromised hosts results in early mortality without ocular involvement (4, 22, 37, 38). Consequently, these studies primarily focused on early and acute responses in fungal endophthalmitis. To mimic a clinical scenario, here, we used the intraperitoneal (i.p.) and intravenous (i.v.) routes for systemic administration of *C. albicans* in immunocompetent mice. Our dose-response and time course studies allowed us to assess innate immune response both at the early (day 1, day 3) and late (day 6) stages of infection. Moreover, because of the immunocompetent status of the mice, our data show that endogenous endophthalmitis can be induced without causing mortality, which is a major advantage of this model. Our survival study showed *C. albicans* was present in the eyes for up to 10 days, whereas it was cleared from most kidneys (primary target organ during candidemia). These results raise the possibility that like viruses (39), eyes might harbor fungal pathogens even though the patient recovered from systemic *C. albicans* infection. However, further investigation is needed to test this hypothesis.

Being a dimorphic fungus, *C. albicans* can exist in its yeast form, which aids in dissemination, and a filamentous form, where it can develop hyphae that can breach and invade tissues (40). During the initial phase of *C. albicans* infection, yeast cells adhere to the epithelium and/or endothelium. As it progresses, hyphal projections are produced, penetrating blood vessels, which ultimately allow it to gain circulatory access (11). Upon systemic candidiasis, the fungus encounters myeloid phagocytes, including neutrophils, inflammatory monocytes, tissue-resident macrophages, and dendritic cells (DCs), which mount strong innate defense (11). These effector cells act by phagocytosis and intracellular killing of *C. albicans* yeast cells by degranulation of antimicrobial molecules and neutrophil extracellular traps (NETs) formation to counteract extracellular fungal hyphae, production of both pro- and anti-inflammatory cytokines, and chemokines, AMPs, hydrolases, and nutritional immunity (41, 42).

The recognition of the *C. albicans* pathogen-associated molecular patterns (PAMPs) by host cell pattern recognition receptors (PRRs) like C-type lectin (CLR) superfamily, including DECTIN-1, -2, and -3, macrophage-inducible C-type lectin (Mincle), and Toll-like receptors (TLRs), triggers the development of an immune response (11, 43). Upon recognition, a signaling cascade involving NF- κ B and mitogen-activated protein kinases (MAPKs) leads to the production of chemokines and cytokines; this allows innate immune sensing and control of *C. albicans* (44). Our data showing the activation of inflammatory signaling with the activation of NF- κ B and ERK, along with induced expression of inflammatory genes in retinal tissues, points to the outcome of *C. albicans* invasion inside the eye, with a similar observation made in *C. albicans*-infected RPE cells. Therefore, the use of MAPK and ERK inhibitors would help in investigating their therapeutic role in preventing *C. albicans* endophthalmitis. In addition to inflammatory mediators, *C. albicans*-infected RPE cells exhibited induced expression of antimicrobial peptides (AMPs) such as beta-defensins and LL-37. These results indicate that RPE cells possess the ability to exert antimicrobial activity via secreted AMPs (11, 45–48). However, similar to our bacterial endophthalmitis study (49), the direct antifungal effects of these AMPs against *C. albicans* need to be investigated. We postulate that the protective response of RPE cells might be the reason for the few cases of ocular candidiasis in immunocompetent individuals. Interestingly, we observed that *C. albicans* induced the expression of fibroblast growth factor 2 (FGF-2), a known enhancer for the virulence of *C. albicans*, which promotes angiogenesis. Thus, blockage of FGF-2 has been proposed as a potential adjunct therapy to treat *C. albicans* infection (50), though further studies are warranted to investigate the role of FGF-2 in *Candida* endogenous endophthalmitis.

Among the various host molecules involved in regulating the inflammatory response against pathogens, our data revealed significant attenuation of AMPK signaling in the *C. albicans*-infected mouse retina and human RPE cells. AMPK is the master regulator of energy homeostasis and cell survival during stress (51, 52), and emerging evidence indicates that AMPK exerts anti-inflammatory effects by inhibiting NF- κ B and other proinflammatory signaling (53). Therefore, upon *C. albicans* infection, reduced AMPK activity may augment the activation of the NF- κ B cascade, leading to persistent inflammatory response in *C. albicans* endophthalmitis. Our prior studies demonstrate an essential role of AMPK in regulating the retinal innate immune response to ocular infection by modulating both residential (glial) and infiltrating immune cells. Therefore, pharmacological AMPK activators such as 5-aminoimidazole-4-carboxamide ribonucleotide (AICAR) and metformin can be potentially used to promote the inflammation resolution in *C. albicans* endogenous endophthalmitis (54–57).

To enter the eye and ultimately cause endophthalmitis, we hypothesize that *C. albicans* must disrupt the blood-retinal barrier (58) composed of retinal vascular endothelium and the retinal pigment epithelium. The retinal pigment epithelium is essential for maintaining the structural and functional integrity of the retina and the outer BRB. RPE cells also act as the first line of defense and express TLRs, complement components, and class I and II major histocompatibility complexes (MHC-I and MHC-II, respectively) and serve as antigen-

presenting cells (59). During an ocular inflammation, the BRB functional state is altered, leading to increased permeability and recruitment of leukocytes in the retinal tissues. Therefore, to further understand the specific role of RPE cells in *C. albicans* invasion, NaIO₃ treatment was utilized as a model for RPE degeneration (60). Our data showing increased *C. albicans* invasion and inflammatory response and reduced ERG function indicate that *C. albicans* causes endogenous endophthalmitis by directly affecting the retinal pigment epithelium. This coincides with similar findings reported in endogenous bacterial endophthalmitis (61). Together, these studies indicate the role of RPE cells in the pathogenesis of endogenous endophthalmitis.

The host response during fungal endophthalmitis leading to loss of BRB integrity is not well defined. Several cellular junction proteins maintain the BRB, and during bacterial infection and other ocular inflammation models (e.g., uveitis and glaucoma), increased inflammatory mediators (e.g., IL-6, MIP2, TNF- α , and IL-1 β) can impair the barrier properties (24, 62–66). The involvement of proinflammatory cytokines and the loss of tight junction protein (ZO-1) have been implicated in endogenous bacterial endophthalmitis (24, 26, 61, 67). Our data using heat-killed *C. albicans* indicate that live *C. albicans* infection is required to disrupt the RPE layer's cell-cell junction integrity, also demonstrated in the case of bacterial endophthalmitis (24). Since AMPK has been shown to play a role in regulating the barrier integrity, we postulate that reduced AMPK levels in our study might be contributing to the breach of outer BRB (57, 68). Hence, our study warrants further in-depth investigation of the role of AMPK in regulating the host response against *C. albicans* endophthalmitis to unravel a novel therapeutic approach to limit ocular candidiasis. Furthermore, apart from the host factors, Sap5p, one of the secreted proteases from *C. albicans*, can directly degrade E-cadherin (69). Therefore, deciphering the role of fungal proteases in disrupting the BRB integrity could provide novel insights into the pathogenesis of fungal endophthalmitis.

This is the first study to distinguish the host factors contributing to inflammation and permeability of the blood-retinal barrier and establish variations in the RPE tight and adherens junctions during fungal endophthalmitis. Our novel findings on the involvement of inflammatory mediators and AMPK in *C. albicans* ocular infection and BRB permeability provide a platform for further studies to comprehend the mechanism of BRB dysfunction and endophthalmitis. In summary, our study provides novel mechanistic insights into both the pathogenesis of *C. albicans* endophthalmitis and the breach of the BRB in fungal endophthalmitis. Moreover, the experimental models developed in this study can be utilized to identify both host and pathogenic factors contributing to the development of endogenous endophthalmitis and also identify therapeutic drugs intended to recover the stability of BRB.

MATERIALS AND METHODS

Mice and ethics statement. C57BL/6J mice (both male and female, 6 to 8 weeks of age) were procured from the Jackson Laboratory (Bar Harbor, ME) and were maintained in the Division of Laboratory Animal Resources (DLAR) facility of the Kresge Eye Institute, Wayne State University. The mice were kept on an alternate 12-h light/dark cycle and fed LabDiet rodent chow (LabDiet, PicoLab, St. Louis, MO, USA). All procedures involving mice were performed as per the Guide for the Care and Use of Laboratory Animals, the Wayne State University IACUC, and the Association for Research in Vision and Ophthalmology Statement for the Use of Animals in Ophthalmic and Vision Research.

***C. albicans* endogenous endophthalmitis model.** *Candida albicans* (strain sc-5314; ATCC) was maintained on yeast extract-peptone-dextrose (YPD) agar plates (Sigma-Aldrich). Prior to mouse inoculation, *C. albicans* was grown at 30°C in YPD broth for 18 h to 24 h, and the infectious dose was adjusted by resuspending in sterile phosphate-buffered saline (PBS) at approximately 2.5×10^6 to 3.5×10^6 CFU/mL. Mice were injected with 200 μ L (i.e., 5×10^5 CFU/mouse) via intraperitoneal or intravenous (lateral tail vein) routes. The eyes were enucleated on days 1, 3, and 6 postinfections for various assays described in the following sections. *C. albicans* was heat killed at 95°C for 10 min followed by plating for confirmation of the process of fungal inactivation.

In vitro outer blood-retinal barrier model. Human retinal pigment epithelial cells (ARPE-19 cell line; ATCC CRL-2302) were maintained in Dulbecco's modified Eagle medium (DMEM)-F-12 culture medium (Invitrogen) supplemented with 10% heat-inactivated fetal bovine serum (FBS; Invitrogen) and 1% penicillin-streptomycin solution (Corning) (70). The cells were grown in a humidified chamber (Thermo Fisher Scientific) at 37°C and 5% CO₂. Cells were challenged with *C. albicans* sc-5314 at various MOIs or time points to perform dose-response and time course studies.

Fungal burden estimation. Mice were euthanized at 1, 3, and 6 days post-*C. albicans* injection, followed by extensive intracardiac perfusion using sterile PBS to remove blood from the circulation. The internal organs (eyes, kidney, spleen, and liver) were aseptically harvested and weighed, and tissue homogenates were prepared using the bead-crushing method. The homogenates were serially diluted in sterile PBS and plated on YPD agar plates (4). The fungal burden was enumerated by CFU count after overnight incubation at 30°C. The fungal burden in infected eyes is expressed as log₁₀ CFU/eye, whereas log₁₀ CFU/g tissue was used for calculation in other organs.

Evans blue permeability assay. The breach of the blood-retinal barrier was quantified after intravenous (i.v.) injection of *C. albicans* using the modified albumin-Evans blue dye extrusion assay as previously described (61). Briefly, *C. albicans* or mock-injected mice were anesthetized with ketamine and xylazine, and albumin-Evans blue dye (30 mg/mL; Sigma-Aldrich) was intravenously administered 2 h prior to euthanasia. Intracardiac perfusion was performed through the left ventricle with saline to remove intravascular albumin-Evans blue. Mice were then euthanized, and organs, including the eye, were harvested, weighed, and suspended in formamide to extract the dye at 55°C for 48 h. The concentration of the dye was measured by spectrophotometer (620 nm absorbance), and values were calculated using a standard curve of albumin-Evans blue dye normalized to the total protein in the sample. The results (mean ± standard error of the mean [SEM]) were expressed as micrograms of dye per milligram of tissue protein content.

ERG analysis. Scotopic electroretinography (ERG) was performed to evaluate retinal visual function in control and *C. albicans*-injected mouse eyes using the Celeris ERG system (Diagnosys LLC, Lowell, MA, USA) as described previously (71). Data were analyzed with respect to control eyes and expressed as percentage of wave amplitude retained.

LDH release assay. The cellular toxicity was performed using LDH release kit as per the manufacturer's instructions (Abcam, CA, USA). Briefly, 10 μL of RPE cell culture supernatant was mixed with kit reagents and incubated for 30 min at room temperature. The LDH activity was quantified using BioTek plate reader at 535/587 nm. The LDH release was normalized compared to the uninfected control and expressed as LDH release (percentage of the age of control).

Real-time PCR. Total RNA was extracted from the retinal tissue or cultured ARPE-19 cells using TRIzol reagent as per the manufacturer's instructions (Invitrogen, Carlsbad, CA, USA). cDNA was synthesized from 1.0 μg of total RNA using a Maxima first-strand cDNA synthesis kit (Thermo Fisher Scientific, Rockford, IL, USA) as per the manufacturer's instructions. The quantitative PCR (qPCR) was performed to assess the expression of genes regulating inflammatory cytokines/chemokines, antimicrobial peptides, and intracellular junction proteins using the StepOnePlus PCR instrument (Applied Biosystems, Grand Island, NY, USA). Gene expression was analyzed by the threshold cycle ($\Delta\Delta C_T$) method and normalized with *Gapdh*, an endogenous housekeeping reference gene.

ELISA. The production of inflammatory cytokines and chemokines was determined using commercially available enzyme-linked immunosorbent assay (ELISA) kits. Twenty micrograms of total protein from whole-eye lysates or 100 μL of the cell culture supernatant were used for individual assays. All ELISAs (TNF-α, IL-1β, IL-6, KC, and CXCL2/MIP2) were performed as per the manufacturer's instructions (R&D Systems, Minneapolis, MN, USA). The data were presented as mean cytokine/chemokine concentrations (picogram per milligram of eye lysates) mean ± SEM for mice and picogram per milliliter (mean ± SD) for cell culture supernatant.

Western blot analysis. For Western blot analyses, hRPE cells were lysed in radioimmunoprecipitation assay (RIPA) lysis buffer (Thermo Scientific), whereas mouse retinal tissue was lysed by sonication in PBS, and the protein concentrations were estimated using the bicinchoninic acid (BCA) assay kit (Thermo Scientific) as per the manufacturer's instructions. Denatured proteins were resolved on 10% sodium dodecyl sulfate-polyacrylamide gel electrophoresis (SDS-PAGE) and transferred onto 0.45-μm nitrocellulose membranes (Bio-Rad, Hercules, CA). The membrane was blocked using 5% nonfat skim milk for whole proteins or in 5% bovine serum albumin (BSA; Sigma-Aldrich) for phosphoproteins, followed by a wash with 1× Tris-glycine buffer with Tween 20 (TBST). Blots were incubated with the primary antibody diluted using 5% BSA in TBST overnight at 4°C with shaking. After secondary antibody incubation, protein bands were visualized using SuperSignal West Femto chemiluminescent substrate (Thermo Scientific, Rockford, IL). For semiquantitative analyses, intensities of protein bands were measured using ImageJ software (NIH, USA).

FITC-dextran permeability assay. The *in vitro* transwell FITC-dextran permeability assay was performed as described previously (72, 73). Briefly, ARPE-19 cells were seeded onto fibronectin (10 μg cm⁻²; Sigma-Aldrich)-coated transwell tissue culture inserts (6.5 mm diameter, 0.4 μm pore size; Corning Costar; catalog no. CLS3470) placed on a 24-well plate. The cell density was 5 × 10⁴ cells per insert, and they were cultured in complete DMEM-F-12 cell growth medium in both upper and lower chambers. Upon confluence (48 h postseeding), cells were infected with *C. albicans* at an MOI of 1 or mock infected. FITC-dextran, 40,000 molecular weight (MW; catalog no. FD40S; Sigma-Aldrich), constituted 150 μL of 1 mg/mL in 1× Hanks' balanced salt solution (HBSS) was added onto the upper chamber, and 600 μL of 1× HBSS was added to the lower chamber. After 1 h of incubation at 37°C, the amount of FITC-dextran permeated into the lower chamber was quantified using absorbance measurement with 490 nm excitation and 530 nm emission (Synergy LX multimode reader). Dextran permeability was expressed as a percentage increase over the basal permeability observed in the mock-infected monolayer at the respective time points. The data are presented as mean ± SD.

Immunofluorescence staining. ARPE-19 cells were cultured in four-well chamber slides (Nunc Lab-Tek) to confluence and allowed to form mature epithelial structures by growing in low-serum media (5% FBS) for 3 days. The confluent monolayer was infected with *C. albicans* at an MOI of 1 for different time

points. The cells were fixed using 4% paraformaldehyde in 1× PBS overnight at 4°C. The cells were washed thrice with 1× PBS and then blocked using 1% BSA in 1× PBS for 1 h at room temperature. The cells were then incubated with rabbit anti-ZO1 IgG (1:100) in the dilution buffer in a humidified chamber overnight at 4°C followed by three washes with 1× PBS. The cells were then incubated with anti-rabbit Alexa Fluor 594 (Invitrogen) for 1 h at room temperature in a humidified chamber. The cells were washed thrice with 1× PBS and mounted in Vectashield antifade mounting medium (Vector Laboratories). The cells were visualized using the Keyence fluorescence microscope at ×600 magnification. The cells with intact peripheral ZO-1 staining were counted against the DAPI (4',6-diamidino-2-phenylindole)-stained cells to detect the nuclei using ImageJ software and represented as cells with ZO-1 staining/DAPI.

Statistical analysis. Statistical analysis was performed using GraphPad Prism 9 software, and the data are presented as mean ± SEM for animal studies or mean ± standard deviation (SD) for *in vitro* studies. A *P* value of <0.05 was considered statistically significant. All experiments were performed at least three times unless mentioned otherwise.

Data availability. The data that support the findings of this study are available from the corresponding author upon reasonable request.

SUPPLEMENTAL MATERIAL

Supplemental material is available online only.

SUPPLEMENTAL FILE 1, PDF file, 0.3 MB.

ACKNOWLEDGMENTS

We thank Robert E. Wright III for the critical reading of the manuscript and for providing technical support for immunostaining experiments.

We report no potential conflict of interest.

This study was supported by National Institutes of Health (NIH) grants R01EY026964 and R01EY027381 to A.K. Our research is also supported in part by an unrestricted grant from Research to Prevent Blindness (RPB) to the Kresge Eye Institute/Department of Ophthalmology, Visual, and Anatomical Sciences and NEI vision center grant P30EY004068. The funders had no role in study design, data collection and interpretation, or the decision to submit the work for publication.

A.K. conceived the idea, and Sn.S. designed the study. Sn.S. and Su.S. performed the experiments and analyzed the data. Sn.S. and A.K. drafted the manuscript. All the authors approved the final version of the manuscript.

REFERENCES

- Durand ML. 2017. Bacterial and fungal endophthalmitis. *Clin Microbiol Rev* 30:597–613. <https://doi.org/10.1128/CMR.00113-16>.
- Sadaka A, Durand ML, Gilmore MS. 2012. Bacterial endophthalmitis in the age of outpatient intravitreal therapies and cataract surgeries: host-microbe interactions in intraocular infection. *Prog Retin Eye Res* 31:316–331. <https://doi.org/10.1016/j.preteyeres.2012.03.004>.
- Deshmukh D, Chakrabarti M, Jayasudha R, Hasnat Ali M, Tyagi M, Sharma S, Joseph J. 2018. Elevated cytokine levels in vitreous as biomarkers of disease severity in infectious endophthalmitis. *PLoS One* 13:e0205292. <https://doi.org/10.1371/journal.pone.0205292>.
- Rottmann BG, Singh PK, Singh S, Revankar SG, Chandrasekar PH, Kumar A. 2020. Evaluation of susceptibility and innate immune response in C57BL/6 and BALB/c mice during *Candida albicans* endophthalmitis. *Invest Ophthalmol Vis Sci* 61:31. <https://doi.org/10.1167/iovs.61.11.31>.
- Dave TV, Dave VP, Sharma S, Karolia R, Joseph J, Pathengay A, Pappuru RR, Das T. 2019. Infectious endophthalmitis leading to evisceration: spectrum of bacterial and fungal pathogens and antibacterial susceptibility profile. *J Ophthalmic Inflamm Infect* 9:9. <https://doi.org/10.1186/s12348-019-0174-y>.
- Kalkanci A, Ozdek S. 2011. Ocular fungal infections. *Curr Eye Res* 36:179–189. <https://doi.org/10.3109/02713683.2010.533810>.
- Oude Lashof AM, Rothova A, Sobel JD, Ruhnke M, Pappas PG, Viscoli C, Schlamm HT, Oborska IT, Rex JH, Kullberg BJ. 2011. Ocular manifestations of candidemia. *Clin Infect Dis* 53:262–268. <https://doi.org/10.1093/cid/cir355>.
- Kato H, Yoshimura Y, Suido Y, Ide K, Sugiyama Y, Matsuno K, Nakajima H. 2018. Prevalence of, and risk factors for, hematogenous fungal endophthalmitis in patients with *Candida* bloodstream infection. *Infection* 46:635–640. <https://doi.org/10.1007/s15010-018-1163-z>.
- Verfaillie C, Weisdorf D, Haake R, Hostetter M, Ramsay NK, McGlave P. 1991. *Candida* infections in bone marrow transplant recipients. *Bone Marrow Transplant* 8:177–184.
- Wisplinghoff H, Bischoff T, Tallent SM, Seifert H, Wenzel RP, Edmond MB. 2004. Nosocomial bloodstream infections in US hospitals: analysis of 24,179 cases from a prospective nationwide surveillance study. *Clin Infect Dis* 39:309–317. <https://doi.org/10.1086/421946>.
- Lopes JP, Lionakis MS. 2022. Pathogenesis and virulence of *Candida albicans*. *Virulence* 13:89–121. <https://doi.org/10.1080/21505594.2021.2019950>.
- Donahue SP, Greven CM, Zuravleff JJ, Eller AW, Nguyen MH, Peacock JE, Jr, Wagener MW, Yu VL. 1994. Intraocular candidiasis in patients with candidemia. Clinical implications derived from a prospective multicenter study. *Ophthalmology* 101:1302–1309. [https://doi.org/10.1016/S0161-6420\(94\)31175-4](https://doi.org/10.1016/S0161-6420(94)31175-4).
- Abe M, Kinjo Y, Ueno K, Takatsuka S, Nakamura S, Ogura S, Kimura M, Araoka H, Sadamoto S, Shinozaki M, Shibuya K, Yoneyama A, Kaku M, Miyazaki Y. 2018. Differences in ocular complications between *Candida albicans* and non-*albicans* *Candida* infection analyzed by epidemiology and a mouse ocular candidiasis model. *Front Microbiol* 9:2477. <https://doi.org/10.3389/fmicb.2018.02477>.
- Chavan R, Mustafa MZ, Narendran N, Tarin S, Yang Y. 2012. A case of *Candida albicans* endophthalmitis with no predisposing risk factors and a distant source of infection. *Case Rep Ophthalmol* 3:277–282. <https://doi.org/10.1159/000342135>.
- Riddell JT, Comer GM, Kauffman C. *albicans*. 2011. Treatment of endogenous fungal endophthalmitis: focus on new antifungal agents. *Clin Infect Dis* 52:648–653. <https://doi.org/10.1093/cid/ciq204>.
- Sallam A, Taylor SR, Khan A, McCluskey P, Lynn WA, Manku K, Pacheco PA, Lightman S. 2012. Factors determining visual outcome in endogenous *Candida* endophthalmitis. *Retina* 32:1129–1134. <https://doi.org/10.1097/IAE.0b013e31822d3a34>.

17. Seidelman J, Fleece M, Bloom A, Lydon E, Yang W, Arnold C, Weber DJ, Okeke NL. 2021. Endogenous *Candida* endophthalmitis: who is really at risk? *J Infect* 82:276–281. <https://doi.org/10.1016/j.jinf.2020.12.032>.
18. Demant E, Easterbrook M. 1977. An experimental model of candida endophthalmitis. *Can J Ophthalmol* 12:304–307.
19. Henderson DK, Edwards JE, Jr., Ishida K, Guze LB. 1979. Experimental hematogenous *Candida* endophthalmitis: diagnostic approaches. *Infect Immun* 23:858–862. <https://doi.org/10.1128/iai.23.3.858-862.1979>.
20. Karagoz E, Ugan RA, Duzgun E, Cadirci E, Keles S, Uyanik MH, Yavan I, Turhan V. 2017. A comparative study of the effects of intravitreal anidulafungin, voriconazole, and amphotericin B in an experimental *Candida* endophthalmitis model. *Curr Eye Res* 42:225–232. <https://doi.org/10.3109/02713683.2016.1170857>.
21. Kocak N, Kaynak S, Kirdar S, Irmak O, Bahar IH. 2009. Comparison of different antifungal treatment regimens for experimental *Candida* endophthalmitis in rabbit models. *Mikrobiyol Bul* 43:619–626. (In Turkish.)
22. Gupta N, Singh PK, Revankar SG, Chandrasekar PH, Kumar A. 2019. Pathobiology of *Aspergillus fumigatus* endophthalmitis in immunocompetent and immunocompromised mice. *Microorganisms* 7:297. <https://doi.org/10.3390/microorganisms7090297>.
23. Singh S, Farr D, Kumar A. 2018. Ocular manifestations of emerging flaviviruses and the blood-retinal barrier. *Viruses* 10:530. <https://doi.org/10.3390/v10100530>.
24. Moyer AL, Ramadan RT, Novosad BD, Astley R, Callegan MC. 2009. *Bacillus cereus*-induced permeability of the blood-ocular barrier during experimental endophthalmitis. *Invest Ophthalmol Vis Sci* 50:3783–3793. <https://doi.org/10.1167/iovs.08-3051>.
25. Hohl TM. 2014. Overview of vertebrate animal models of fungal infection. *J Immunol Methods* 410:100–112. <https://doi.org/10.1016/j.jim.2014.03.022>.
26. Kumar A, Kumar A. 2015. Role of *Staphylococcus aureus* virulence factors in inducing inflammation and vascular permeability in a mouse model of bacterial endophthalmitis. *PLoS One* 10:e0128423. <https://doi.org/10.1371/journal.pone.0128423>.
27. Wang J, Iacovelli J, Spencer C, Saint-Geniez M. 2014. Direct effect of sodium iodate on neurosensory retina. *Invest Ophthalmol Vis Sci* 55:1941–1953. <https://doi.org/10.1167/iovs.13-13075>.
28. Hanus J, Anderson C, Sarraf D, Ma J, Wang S. 2016. Retinal pigment epithelial cell necrosis in response to sodium iodate. *Cell Death Discov* 2:16054. <https://doi.org/10.1038/cddiscovery.2016.54>.
29. Moriguchi M, Nakamura S, Inoue Y, Nishinaka A, Nakamura M, Shimazawa M, Hara H. 2018. Irreversible photoreceptors and RPE cells damage by intravenous sodium iodate in mice is related to macrophage accumulation. *Invest Ophthalmol Vis Sci* 59:3476–3487. <https://doi.org/10.1167/iovs.17-23532>.
30. Kiuchi K, Yoshizawa K, Shikata N, Moriguchi K, Tsubura A. 2002. Morphologic characteristics of retinal degeneration induced by sodium iodate in mice. *Curr Eye Res* 25:373–379. <https://doi.org/10.1076/ceyr.25.6.373.14227>.
31. Tamai R, Kiyoura Y. 2019. Heat-killed *Candida albicans* augments synthetic bacterial component-induced proinflammatory cytokine production. *Folia Microbiol (Praha)* 64:555–566. <https://doi.org/10.1007/s12223-019-00679-2>.
32. Naglik JR, Challacombe SJ, Hube B. 2003. *Candida albicans* secreted aspartyl proteinases in virulence and pathogenesis. *Microbiol Mol Biol Rev* 67:400–428. <https://doi.org/10.1128/MMBR.67.3.400-428.2003>.
33. Yapar N. 2014. Epidemiology and risk factors for invasive candidiasis. *Ther Clin Risk Manag* 10:95–105. <https://doi.org/10.2147/TCRM.S40160>.
34. Deren YT, Ozdek S, Kalkan A, Akyurek N, Hasanreisoglu B. 2010. Comparison of antifungal efficacies of moxifloxacin, liposomal amphotericin B, and combination treatment in experimental *Candida albicans* endophthalmitis in rabbits. *Can J Microbiol* 56:1–7. <https://doi.org/10.1139/w09-112>.
35. Arikan S, Ozdek S, Aktas Z, Dincel A, Hasanreisoglu B. 2013. Vitreous and aqueous penetration of intravitreally and orally administered moxifloxacin in an experimental rabbit model of fungal endophthalmitis. *J Pharm Pharmacol* 65:659–664. <https://doi.org/10.1111/jphp.12029>.
36. Gupta SK, Dhingra N, Velpandian T, Jaiswal J. 2000. Efficacy of fluconazole and liposome entrapped fluconazole for *C. albicans* induced experimental mycotic endophthalmitis in rabbit eyes. *Acta Ophthalmol Scand* 78:448–450. <https://doi.org/10.1034/j.1600-0420.2000.078004448.x>.
37. Guest JM, Singh PK, Revankar SG, Chandrasekar PH, Kumar A. 2018. Isavuconazole for treatment of experimental fungal endophthalmitis caused by *Aspergillus fumigatus*. *Antimicrob Agents Chemother* 62:e01537-18. <https://doi.org/10.1128/AAC.01537-18>.
38. Conti HR, Huppler AR, Whibley N, Gaffen SL. 2014. Animal models for candidiasis. *Curr Protoc Immunol* 105:19.16.11–19.16.17. <https://doi.org/10.1002/0471142735.im1906s105>.
39. Smith JR, Todd S, Ashander LM, Charitou T, Ma Y, Yeh S, Crozier I, Michael MZ, Appukuttan B, Williams KA, Lynn DJ, Marsh GA. 2017. Retinal pigment epithelial cells are a potential reservoir for Ebola virus in the human eye. *Transl Vis Sci Technol* 6:12. <https://doi.org/10.1167/tvst.6.4.12>.
40. Mayer FL, Wilson D, Hube B. 2013. *Candida albicans* pathogenicity mechanisms. *Virulence* 4:119–128. <https://doi.org/10.4161/viru.22913>.
41. Urban CF, Ermert D, Schmid M, Abu-Abed U, Goosmann C, Nacken W, Brinkmann V, Jungblut PR, Zychlinsky A. 2009. Neutrophil extracellular traps contain calprotectin, a cytosolic protein complex involved in host defense against *Candida albicans*. *PLoS Pathog* 5:e1000639. <https://doi.org/10.1371/journal.ppat.1000639>.
42. Urban CF, Backman E. 2020. Eradicating, retaining, balancing, swarming, shuttling and dumping: a myriad of tasks for neutrophils during fungal infection. *Curr Opin Microbiol* 58:106–115. <https://doi.org/10.1016/j.mib.2020.09.011>.
43. Hardison SE, Brown GD. 2012. C-type lectin receptors orchestrate antifungal immunity. *Nat Immunol* 13:817–822. <https://doi.org/10.1038/ni.2369>.
44. Bohringer M, Pohlers S, Schulze S, Albrecht-Eckardt D, Piegsa J, Weber M, Martin R, Hunniger K, Linde J, Guthke R, Kurzai O. 2016. *Candida albicans* infection leads to barrier breakdown and a MAPK/NF-kappaB mediated stress response in the intestinal epithelial cell line C2BBE1. *Cell Microbiol* 18:889–904. <https://doi.org/10.1111/cmi.12566>.
45. Tsai PW, Yang CY, Chang HT, Lan CY. 2011. Human antimicrobial peptide LL-37 inhibits adhesion of *Candida albicans* by interacting with yeast cell-wall carbohydrates. *PLoS One* 6:e17755. <https://doi.org/10.1371/journal.pone.0017755>.
46. Lopez-Garcia B, Lee PH, Yamasaki K, Gallo RL. 2005. Anti-fungal activity of cathelicidins and their potential role in *Candida albicans* skin infection. *J Invest Dermatol* 125:108–115. <https://doi.org/10.1111/j.0022-202X.2005.23713.x>.
47. den Hertog AL, van Marle J, van Veen HA, Van't Hof W, Bolscher JG, Veerman EC, Nieuw Amerongen AV. 2005. Candidacidal effects of two antimicrobial peptides: histatin 5 causes small membrane defects, but LL-37 causes massive disruption of the cell membrane. *Biochem J* 388:689–695. <https://doi.org/10.1042/BJ20042099>.
48. Vylkova S, Nayyar N, Li W, Edgerton M. 2007. Human beta-defensins kill *Candida albicans* in an energy-dependent and salt-sensitive manner without causing membrane disruption. *Antimicrob Agents Chemother* 51:154–161. <https://doi.org/10.1128/AAC.00478-06>.
49. Shamsuddin N, Kumar A. 2011. TLR2 mediates the innate response of retinal Muller glia to *Staphylococcus aureus*. *J Immunol* 186:7089–7097. <https://doi.org/10.4049/jimmunol.1100565>.
50. Vellanki S, Huh EY, Saville SP, Lee SC. 2019. *Candida albicans* morphology-dependent host FGF-2 response as a potential therapeutic target. *J Fungi (Basel)* 5:22. <https://doi.org/10.3390/jof5010022>.
51. Hardie DG, Schaffer BE, Brunet A. 2016. AMPK: an energy-sensing pathway with multiple inputs and outputs. *Trends Cell Biol* 26:190–201. <https://doi.org/10.1016/j.tcb.2015.10.013>.
52. Hardie DG, Ross FA, Hawley SA. 2012. AMPK: a nutrient and energy sensor that maintains energy homeostasis. *Nat Rev Mol Cell Biol* 13:251–262. <https://doi.org/10.1038/nrm3311>.
53. Salminen A, Hyttinen JM, Kaarniranta K. 2011. AMP-activated protein kinase inhibits NF-kappaB signaling and inflammation: impact on healthspan and lifespan. *J Mol Med (Berl)* 89:667–676. <https://doi.org/10.1007/s00109-011-0748-0>.
54. Zhang BB, Zhou G, Li C. 2009. AMPK: an emerging drug target for diabetes and the metabolic syndrome. *Cell Metab* 9:407–416. <https://doi.org/10.1016/j.cmet.2009.03.012>.
55. Singh S, Singh PK, Suhail H, Arumugaswami V, Pellett PE, Giri S, Kumar A. 2020. AMP-activated protein kinase restricts Zika virus replication in endothelial cells by potentiating innate antiviral responses and inhibiting glycolysis. *J Immunol* 204:1810–1824. <https://doi.org/10.4049/jimmunol.1901310>.
56. Kumar A, Giri S, Kumar A. 2016. 5-Aminoimidazole-4-carboxamide ribonucleoside-mediated adenosine monophosphate-activated protein kinase activation induces protective innate responses in bacterial endophthalmitis. *Cell Microbiol* 18:1815–1830. <https://doi.org/10.1111/cmi.12625>.
57. Asgharzadeh F, Barneh F, Fakhraie M, Adel Barkhordar SL, Shabani M, Soleimani A, Rahmani F, Ariakia F, Mehraban S, Avan A, Hashemzahi M, Arjmand MH, Behnam-Rassouli R, Jafari N, Sayyed-Hosseini SH, Ferns GA, Ryzhikov M, Jafari M, Khazaei M, Hassanian SM. 2021. Metformin

- inhibits polyphosphate-induced hyper-permeability and inflammation. *Int Immunopharmacol* 99:107937. <https://doi.org/10.1016/j.intimp.2021.107937>.
58. Lavine JA, Mititelu M. 2015. Multimodal imaging of refractory *Candida* chorioretinitis progressing to endogenous endophthalmitis. *J Ophthalmic Inflamm Infect* 5:54. <https://doi.org/10.1186/s12348-015-0054-z>.
 59. Kumar MV, Nagineni CN, Chin MS, Hooks JJ, Detrick B. 2004. Innate immunity in the retina: Toll-like receptor (TLR) signaling in human retinal pigment epithelial cells. *J Neuroimmunol* 153:7–15. <https://doi.org/10.1016/j.jneuroim.2004.04.018>.
 60. Machalińska A, Lubiński W, Klos P, Kawa M, Baumert B, Penkala K, Grzegorzóka R, Karczewicz D, Wiszniewska B, Machaliński B. 2010. Sodium iodate selectively injures the posterior pole of the retina in a dose-dependent manner: morphological and electrophysiological study. *Neurochem Res* 35:1819–1827. <https://doi.org/10.1007/s11064-010-0248-6>.
 61. Coburn PS, Wiskur BJ, Miller FC, LaGrow AL, Astley RA, Elliott MH, Callegan MC. 2016. Bloodstream-to-eye infections are facilitated by outer blood-retinal barrier dysfunction. *PLoS One* 11:e0154560. <https://doi.org/10.1371/journal.pone.0154560>.
 62. Ramadan RT, Moyer AL, Callegan MC. 2008. A role for tumor necrosis factor-alpha in experimental *Bacillus cereus* endophthalmitis pathogenesis. *Invest Ophthalmol Vis Sci* 49:4482–4489. <https://doi.org/10.1167/iovs.08-2085>.
 63. De Vos AF, Van Haren MA, Verhagen C, Hoekzema R, Kijlstra A. 1995. Systemic anti-tumor necrosis factor antibody treatment exacerbates endotoxin-induced uveitis in the rat. *Exp Eye Res* 61:667–675. [https://doi.org/10.1016/S0014-4835\(05\)80017-X](https://doi.org/10.1016/S0014-4835(05)80017-X).
 64. Luna JD, Chan CC, Derevjanić NL, Mahlow J, Chiu C, Peng B, Tobe T, Campochario PA, Viores SA. 1997. Blood-retinal barrier (BRB) breakdown in experimental autoimmune uveoretinitis: comparison with vascular endothelial growth factor, tumor necrosis factor alpha, and interleukin-1beta-mediated breakdown. *J Neurosci Res* 49:268–280. [https://doi.org/10.1002/\(SICI\)1097-4547\(19970801\)49:3%3C268::AID-JNR2%3E3.0.CO;2-A](https://doi.org/10.1002/(SICI)1097-4547(19970801)49:3%3C268::AID-JNR2%3E3.0.CO;2-A).
 65. Bamforth SD, Lightman S, Greenwood J. 1996. The effect of TNF-alpha and IL-6 on the permeability of the rat blood-retinal barrier in vivo. *Acta Neuropathol* 91:624–632. <https://doi.org/10.1007/s004010050476>.
 66. Mangan BG, Al-Yahya K, Chen CT, Gionfriddo JR, Powell CC, Dubielzig RR, Ehrhart EJ, Madl JE. 2007. Retinal pigment epithelial damage, breakdown of the blood-retinal barrier, and retinal inflammation in dogs with primary glaucoma. *Vet Ophthalmol* 10(Suppl 1):117–124. <https://doi.org/10.1111/j.1463-5224.2007.00585.x>.
 67. Coburn PS, Wiskur BJ, Astley RA, Callegan MC. 2015. Blood-retinal barrier compromise and endogenous *Staphylococcus aureus* endophthalmitis. *Invest Ophthalmol Vis Sci* 56:7303–7311. <https://doi.org/10.1167/iovs.15-17488>.
 68. Sun X, Yang Q, Rogers CJ, Du M, Zhu MJ. 2017. AMPK improves gut epithelial differentiation and barrier function via regulating Cdx2 expression. *Cell Death Differ* 24:819–831. <https://doi.org/10.1038/cdd.2017.14>.
 69. Villar CC, Kashleva H, Nobile CJ, Mitchell AP, Dongari-Bagtzoglou A. 2007. Mucosal tissue invasion by *Candida albicans* is associated with E-cadherin degradation, mediated by transcription factor Rim101p and protease Sap5p. *Infect Immun* 75:2126–2135. <https://doi.org/10.1128/IAI.00054-07>.
 70. Singh PK, Guest JM, Kanwar M, Boss J, Gao N, Juzych MS, Abrams GW, Yu FS, Kumar A. 2017. Zika virus infects cells lining the blood-retinal barrier and causes chorioretinal atrophy in mouse eyes. *JCI Insight* 2:e92340. <https://doi.org/10.1172/jci.insight.92340>.
 71. Das S, Singh S, Kumar A. 2021. Bacterial burden declines but neutrophil infiltration and ocular tissue damage persist in experimental *Staphylococcus epidermidis* endophthalmitis. *Front Cell Infect Microbiol* 11:780648. <https://doi.org/10.3389/fcimb.2021.780648>.
 72. Singh S, Anupriya MG, Modak A, Sreekumar E. 2018. Dengue virus or NS1 protein induces trans-endothelial cell permeability associated with VE-Cadherin and RhoA phosphorylation in HMEC-1 cells preventable by Angiopoietin-1. *J Gen Virol* 99:1658–1670. <https://doi.org/10.1099/jgv.0.001163>.
 73. Anupriya MG, Singh S, Hulyalkar NV, Sreekumar E. 2018. Sphingolipid signaling modulates trans-endothelial cell permeability in dengue virus infected HMEC-1 cells. *Prostaglandins Other Lipid Mediat* 136:44–54. <https://doi.org/10.1016/j.prostaglandins.2018.05.001>.